The Effects of the Failure Diameter of an Explosive on Its Response to Shaped-Charge Jet Attack

by William Lawrence
and John Starkenberg

19970523 049

Army Research Laboratory

Aberdeen Proving Ground, MD 21005-5066

The Effects of the Failure Diameter of an Explosive on Its Response to Shaped-Charge Jet Attack

William Lawrence, John Starkenberg
Weapons and Materials Research Directorate, ARL

Abstract

In order to shed some light on the response of explosives to the attack of small-diameter projectiles such as shaped-charge jets, a computational study using the 2DE code and the Forest Fire explosive initiation model for Composition B was conducted. In our computations we modeled the jet as a cylindrical projectile with a flat end that moves without stretching. Jet attack simulations were run in order to determine modes of initiation and critical velocity for initiation as a function of jet diameter. The diameter of the jet was varied between 0.3 and 12.0 mm. The velocity of the jet was varied between 0.8 and 15.0 km/s. The target diameter was at least three times the jet diameter, and the target was between 4 and 60 jet diameters deep. Two modes of initiation associated with shaped-charge jet attack were observed. Prompt impact-mode initiation occurred for both subsonic and supersonic penetration. Delayed penetration-mode initiation occurred only for supersonic penetration. The velocity threshold for large subsonic jets agreed with the Jacobs-Roslund fit. For jets with diameters smaller than the failure diameter of the explosive they attack, higher velocities than predicted by Jacobs-Roslund were required for initiation. A critical boundary between impact- and penetration-mode initiation was determined over the entire supersonic range. A similar boundary between penetration mode initiation and initiation failure for 0.3-mm and 1.5-mm-diameter jets was found, but the initiation failure threshold for other jet diameters has not yet been determined.

TABLE OF CONTENTS

INTENTIONALLY LEFT BLANK.

LIST OF FIGURES

1. INTRODUCTION

The response of high explosives to projectile impact is of considerable importance in assessing the vulnerability of munitions. Their response, when impacted by small high-speed projectiles such as shaped-charge jets, is of particular interest. The diameters of these jets are usually smaller than the critical diameters required for propagation of detonation in the energetic materials they might be expected to attack. Conditions required for shock-to-detonation transition following the impact of projectiles having diameters larger than the explosive's failure diameter have been well characterized [1] and are described by an empirical relationship commonly known as the Jacobs-Roslund formula. Studies by Chick et al. [2] indicate that alternate modes of response may prevail under other conditions. In some cases, they observed delayed initiation emanating from the bow wave produced by supersonic jet penetration, rather than prompt initiation associated with the initial impact of the jet.

The basic mechanism for shock initiation of detonation in heterogeneous explosives is shock interactions at density discontinuities that produce local hot spots leading to decomposition. The shock magnitude and duration are very important in controlling buildup to detonation. Once an explosive has been initiated, the detonation wave will continue to propagate throughout the charge only if the diameter of the initiated region is sufficient. If it is smaller than that required to maintain a propagating detonation, rarefactions will dominate the flow and restrict reaction to that directly driven by the projectile. This suggests that jet diameter and penetration velocity are the main parameters controlling the initiation process. Larger jet diameters produce broader bow waves that are less susceptible to rarefactions and, therefore, more effective in initiating the explosive.

In order to shed some light on the response of explosives to the attack of small-diameter projectiles and to explain some of Chick's observations, a computational study was conducted using the 2DE code and the Forest Fire explosive initiation model for Composition B. The results reported here are limited to attack against bare explosive. The response of covered explosive is somewhat different and has been discussed by Frey et al. [3] using nonreactive computations.

1

2. DESCRIPTIONS OF 2DE AND FOREST FIRE

The 2DE code is a two-dimensional Eulerian finite-difference hydrocode for solving continuum mechanics problems [4]. It was developed at the Los Alamos Scientific Laboratory for application to explosive initiation problems. The code makes use of the HOM equation of state, the C-J Volume Burn model for detonation propagation, and the Forest Fire explosive initiation model [5], which may also be used for detonation propagation. Chemical reaction is described by a single-reaction progress variable, the unreacted mass fraction, which varies from 1 in the unreacted state to 0 in the completely reacted state. Shock and detonation waves are treated using the method of artificial viscosity.

Forest Fire is a reaction-rate model that predicts the response of explosives to loading by sustained shock waves. The reaction rate is given as a function of the pressure. The model is empirical and relates each explosive's reaction rate to simple sensitivity data characterizing that explosive collected in the wedge test. Wedge-test data is typically summarized in a plot of distance of run to detonation as a function of initial shock pressure known as the "Pop plot" [6]. Forest Fire is derived so as to reproduce this behavior.

This work represents our last use of 2DE. Future investigations will be carried out using the CTH code with the History Variable Reactive Burn (HVRB) explosive initiation model because it offers more versatile problem configuration options, more realistic constitutive models, and a more accurate reaction model.

3. JET AND TARGET DESCRIPTION

Shaped-charge jets have a very complicated structure. They may be continuous or discontinuous (particulated). The material velocity in continuous jets generally decreases from tip to tail producing a stretching jet. Particulated jets consist of numerous fragments with velocities decreasing from very high values at the jet tip. In our computations, we represented the jet as a flat-tipped, cylindrical projectile that does not stretch. We used jets with diameters varying from

0.3 mm to 12.0 mm and velocities varying from 15.0 km/s to 0.8 km/s. The target was always bare Composition B, simulated as a cylinder of varying depth and diameter. The jet and target configurations were varied in accordance with a scheme designed to limit the total number of zones required by a computation while observing a previously determined zone-size constraint based on convergence of solutions for critical diameter. The length of the jet was adjusted in order to conform to the requirements of the scheme.

4. INITIATION OF COMPOSITION B BY JET ATTACK

Jet-attack simulations were run in order to determine modes of initiation and critical velocity for initiation as a function of jet diameter. We observed two modes of initiation in the computations: impact and penetration. The impact mode is typical of large-diameter jets at subsonic penetration velocities. In this case, initiation appears promptly at the impact shock front and detonation spreads from the impact point. If the jet velocity is too low to produce initiation, the impact shock wave propagates away from the subsonic jet tip. In the case of supersonic penetration, a bow wave develops after impact. The ambient sound speed in inert Composition B, as given in the equation-of-state hugoniot, is about 2.3 km/s, and the jet velocity producing sonic penetration in bare Composition B is about 3.3 km/s. With small-diameter jets penetrating at supersonic velocities, we observed impact-mode initiation at the highest jet velocities and penetration-mode initiation at somewhat lower velocities. When the jet velocity was further reduced, no initiation was observed. However, in the case of supersonic penetration, we have classified such responses as indeterminate either because the jet was fully consumed or because it appeared that further penetration might still produce initiation. Impact-mode initiation is not affected by the assumption of a nonstretching jet. However, penetration-mode initiation can be further delayed or eliminated by the decrease in penetration velocity with depth of penetration associated with a stretching jet.

Visualization of the results is facilitated by plotting contours of reactant mass fraction at various times. Detonation is identified as a region of closely spaced contours. These plots also show the interfaces between the air, solid explosive, and reaction products. Pressure histories at Lagrangian stations are also useful.

3

Impact- and penetration-mode initiation have been observed for a 1.5-mm-diameter jet and are shown in Figures 1–3. Figure 1 shows a sequence of mass fraction contour plots for an impact-mode initiation. After a short distance of run, the mass fraction contours become closely spaced near the axis, indicating that buildup to detonation has occurred. As the jet penetrates, the diameter of the burned explosive region increases, briefly decreases, and then increases again, spreading across the entire charge. Pressure histories were also computed at various locations in the explosive. A pressure history for 1.5-mm-diameter jet impacting Composition B at a velocity of 5.2 km/s at one location is shown in Figure 2. This figure shows a peak pressure of more than 37 Gpa. This is much more than the pressure required to detonate Composition B. Figure 3 shows a sequence of similar plots for a delayed or penetration-mode initiation. The mass fraction contours remain spread out for a long period of time. They gradually converge and become closely spaced only after the jet penetrates some 30 mm into the explosive (about 6 μs after impact). The detonation then propagates away from the jet tip into the remainder of the charge. Pressure histories in the explosive, at various locations along the axis of symmetry, are presented in Figure 4. This figure shows that the growth of the bow shock to detonation started between 5 μs and 6 μs. Indeterminate responses were observed when the jet velocity was decreased to 4.9 mm/μs and lower. Figure 5 shows a sequence of mass fraction contour plots for impact of a 4.7-mm/μs jet in which the jet is entirely eroded by the end of the computation.

Figure 6 shows a sequence of mass fraction contour plots for the impact of 0.3-mm-diameter jet at 12.0 mm/μs. The explosive started to detonate immediately on impact and the diameter of the front increased with penetration. This is characteristic of an impact-mode initiation. When the velocity of the same jet was decreased to 10.0 mm/μs, the explosive did not detonate prior to complete erosion of the jet and nearly complete penetration of the target as shown in Figure 7. In this case, it appears that the mass fraction contours are broadening and that deeper penetration might still produce initiation. These problems can better be handled by a more modern code like CTH, which allows mass to be fed in at the boundaries.

Impact-mode initiation and initiation failure have also been determined for subsonic penetration projectiles. Figure 8 shows mass fraction contour plots for impact-mode initiation with a 5-mm-diameter jet at 1.65 mm/μs. Pressure histories were computed inside the explosive

Figure 1. Mass fraction contour plots showing impact-mode initiation following the impact of 1.5-mm-diameter jet at 5.2 mm/μs.

at various locations along the axis of symmetry as shown in Figure 9. This shows that the shock pressure increased to detonation pressure immediately. In the case of subsonic penetration, initiation failure is easy to identify as the impact shock wave moves rapidly away from the jet tip and the region of reaction. Figure 10 shows this initiation failure for the same jet at 1.5 mm/μs.
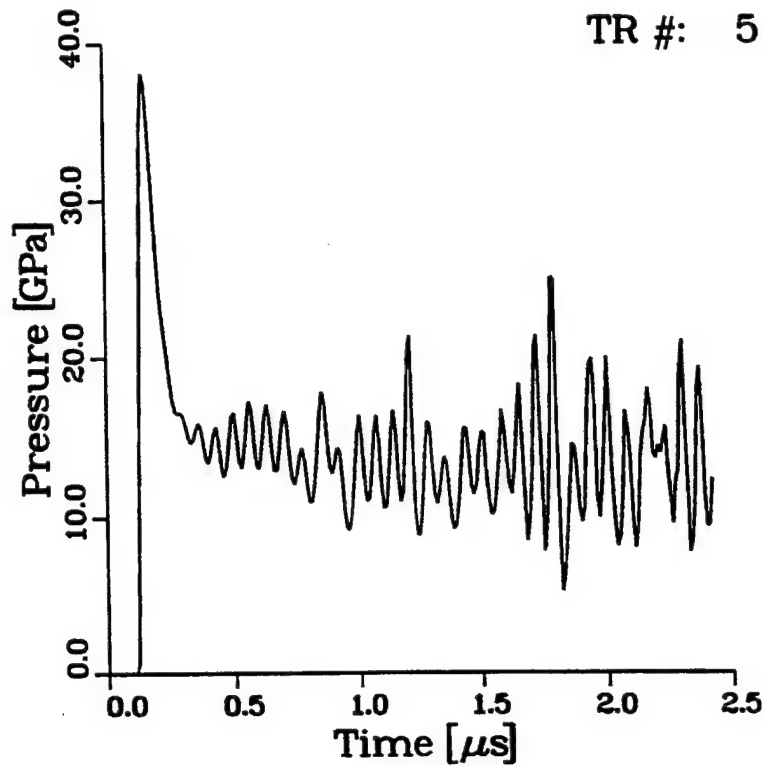
Figure 2. Pressure history for impact-mode initiation with 1.5-mm-diameter jet at 5.2 mm/μs.

Jet diameter, jet impact velocity, steady-state penetration velocity of the jet, and the modes of initiation of the explosive are given in Table 1. The computations for jets of different diameters and impact velocities were made, and the mass fraction contours are shown in the Appendix.

Critical jet velocity for initiation of Composition B increases as the jet diameter decreases. Figure 11 shows a plot of the critical velocities vs. the ratio of jet diameter to Composition B failure diameter (~4 mm). Results for jet diameters greater than the failure diameter ($d_j/d_f > 1.0$) are from computations made a number of years ago [7]. The present computations extend these results to jets with diameters as small as 0.3 mm. For jets penetrating at subsonic speeds having diameters greater than the explosive's failure diameter, we have determined a critical velocity whose dependence on jet diameter agrees with the Jacobs-Roslund fit ($v_j^2 d_j = 10.6$ mm^3/μs^2, effectively
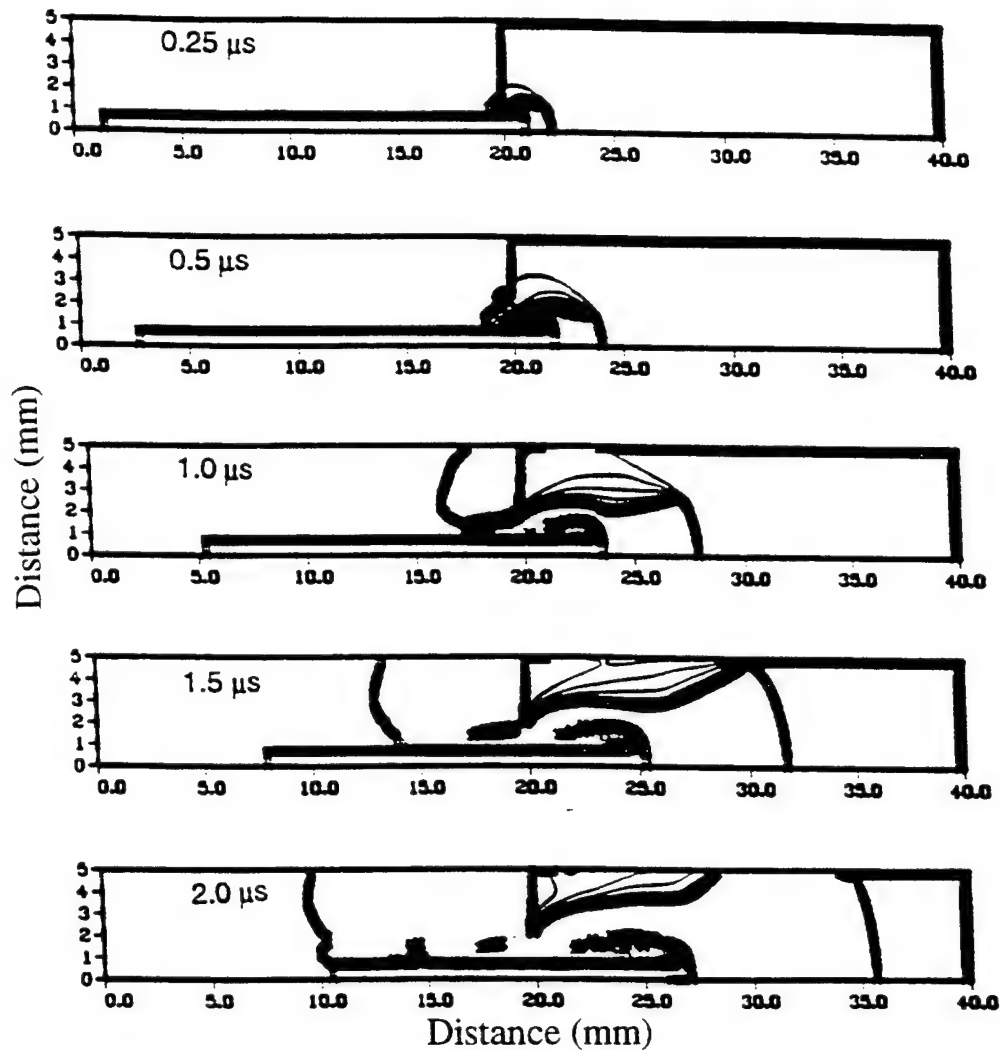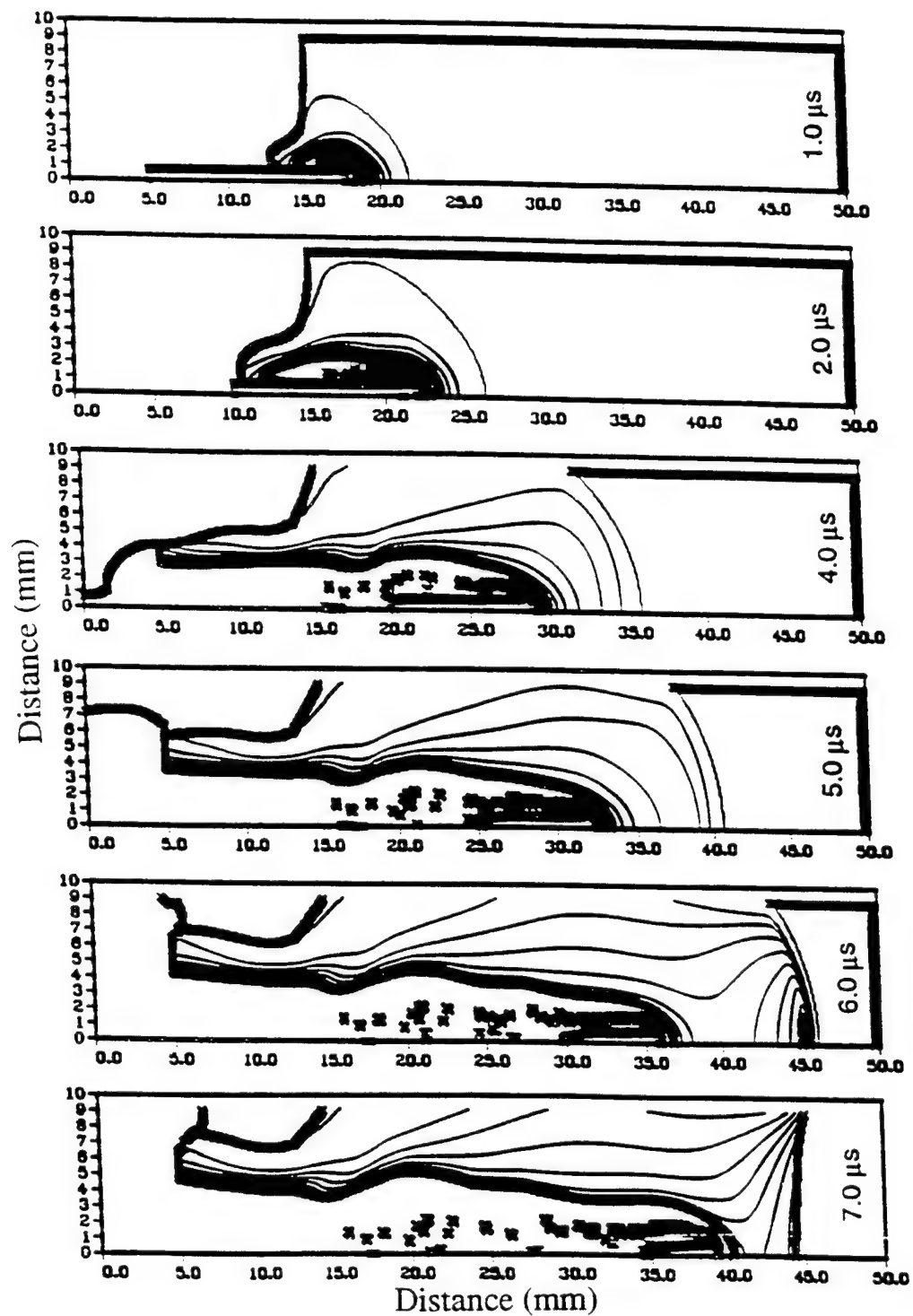
Figure 3. Mass fraction contour plots showing penetration-mode initiation following the impact of 1.5-mm-diameter jet at 5.0 mm/μs.
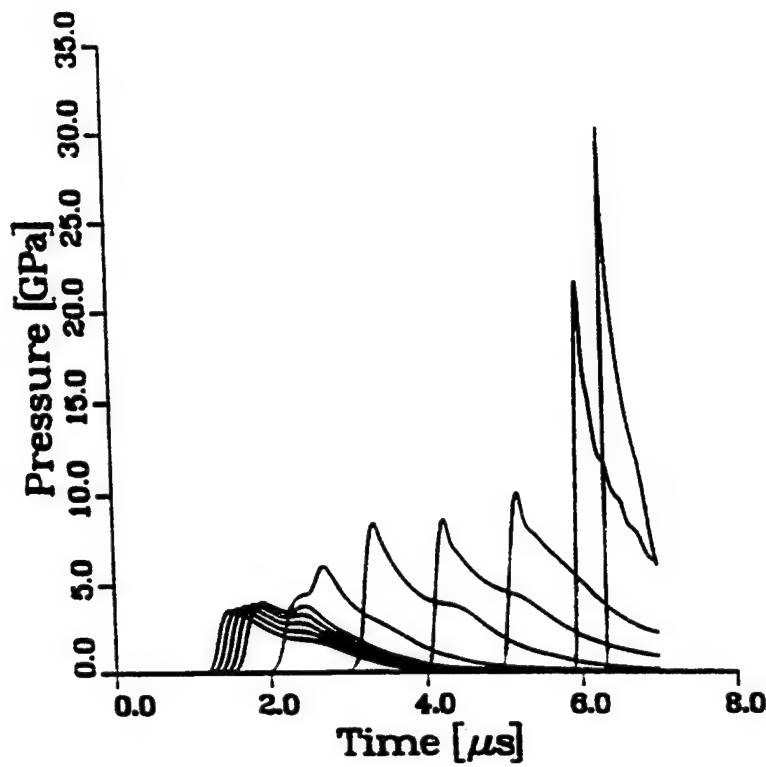
Figure 4. Pressure history for penetration-mode initiation following the impact of 1.5-mm-diameter jet at 5.0 mm/μs.

representing experimental data for projectile diameters larger than 6.0 mm). As the jet diameter decreases below the failure diameter, however, it becomes increasingly difficult to initiate the explosive. The critical velocity increases with decreasing jet diameter more rapidly than the Jacobs-Roslund formula suggests. Jets having diameters below about 2.0 mm must penetrate at supersonic speeds in order to produce initiation. In this case, a critical boundary between impact- and penetration-mode initiations has been determined. A critical boundary dividing penetration-mode initiation from initiation failure has not been determined.

Lundstrom [8] reported results from similar computations with short projectiles. His results predict somewhat higher critical velocities, so a 2-mm-diameter projectile, for example, would require supersonic penetration to produce initiation. His computation for 2-mm-diameter

8

Figure 5. Mass fraction contour plots showing the indeterminate response following the impact of 1.5-mm-diameter jet at 4.7 mm/μs.

9
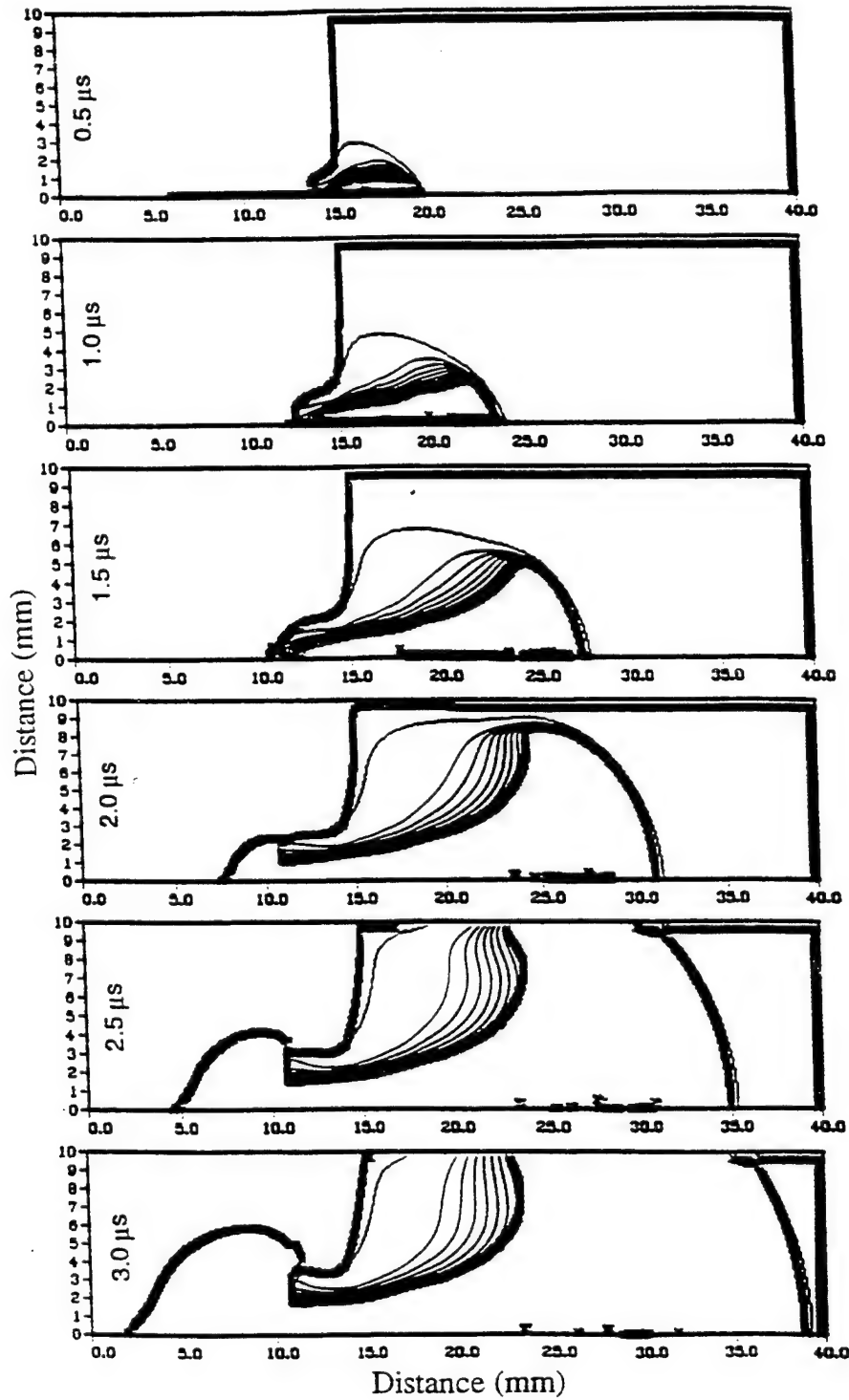
Figure 6. Mass fraction contour plots showing impact-mode initiation following the impact of 0.3-mm-diameter jet at 12.0 mm/μs.

10

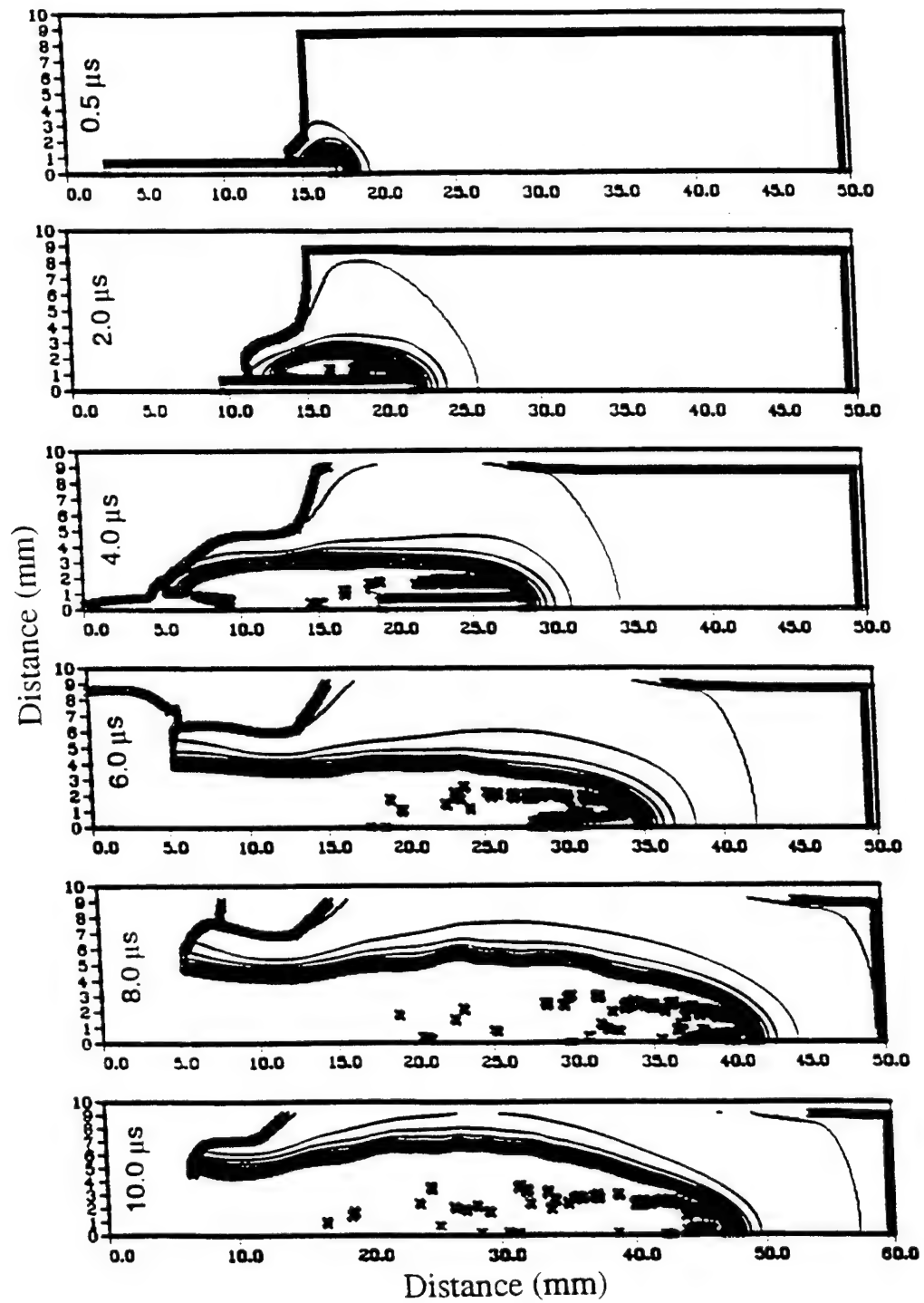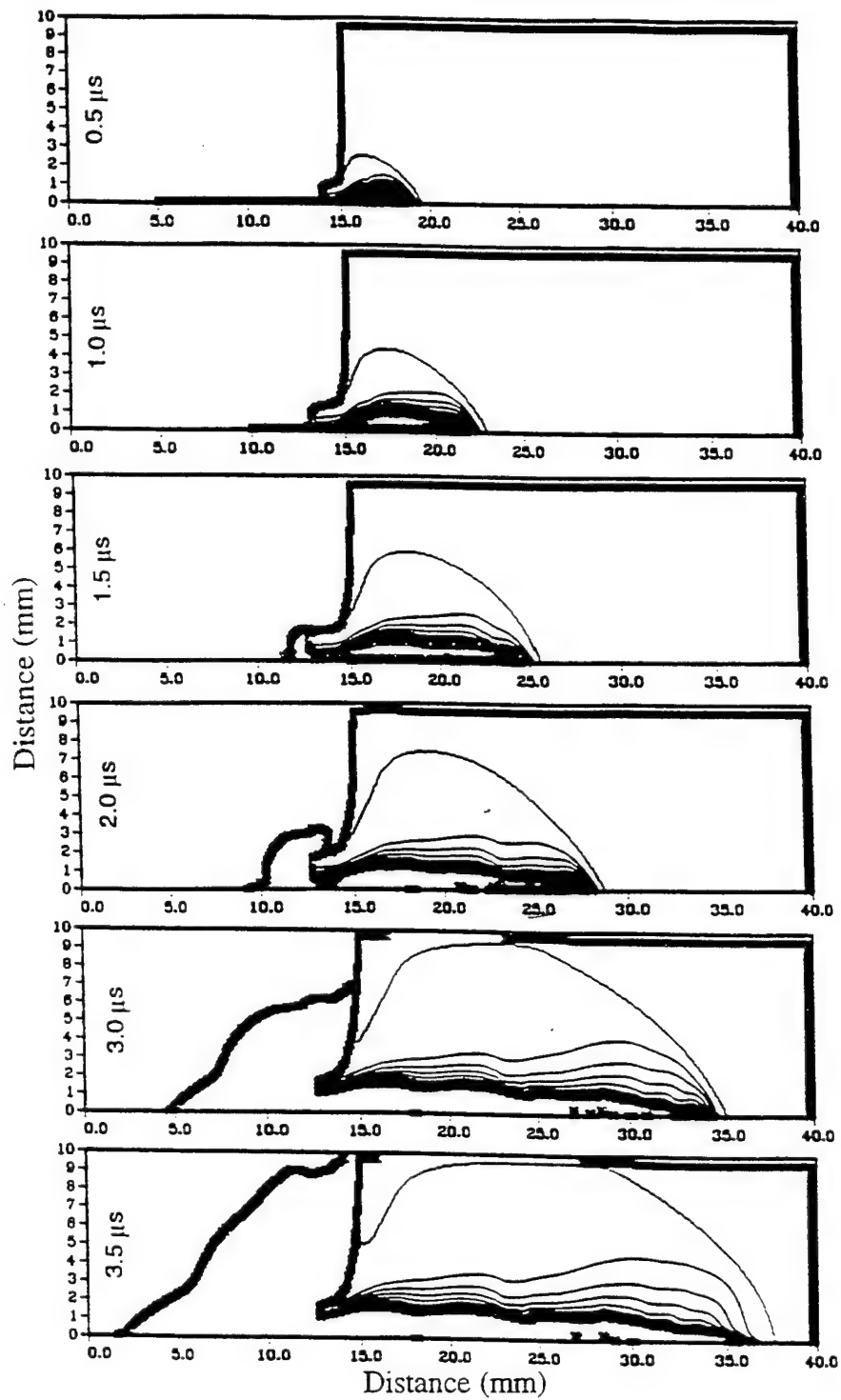Figure 7. Mass fraction contour plots showing indeterminate response following the impact of 0.3-mm-diameter jet at 10.0 mm/µs.

11
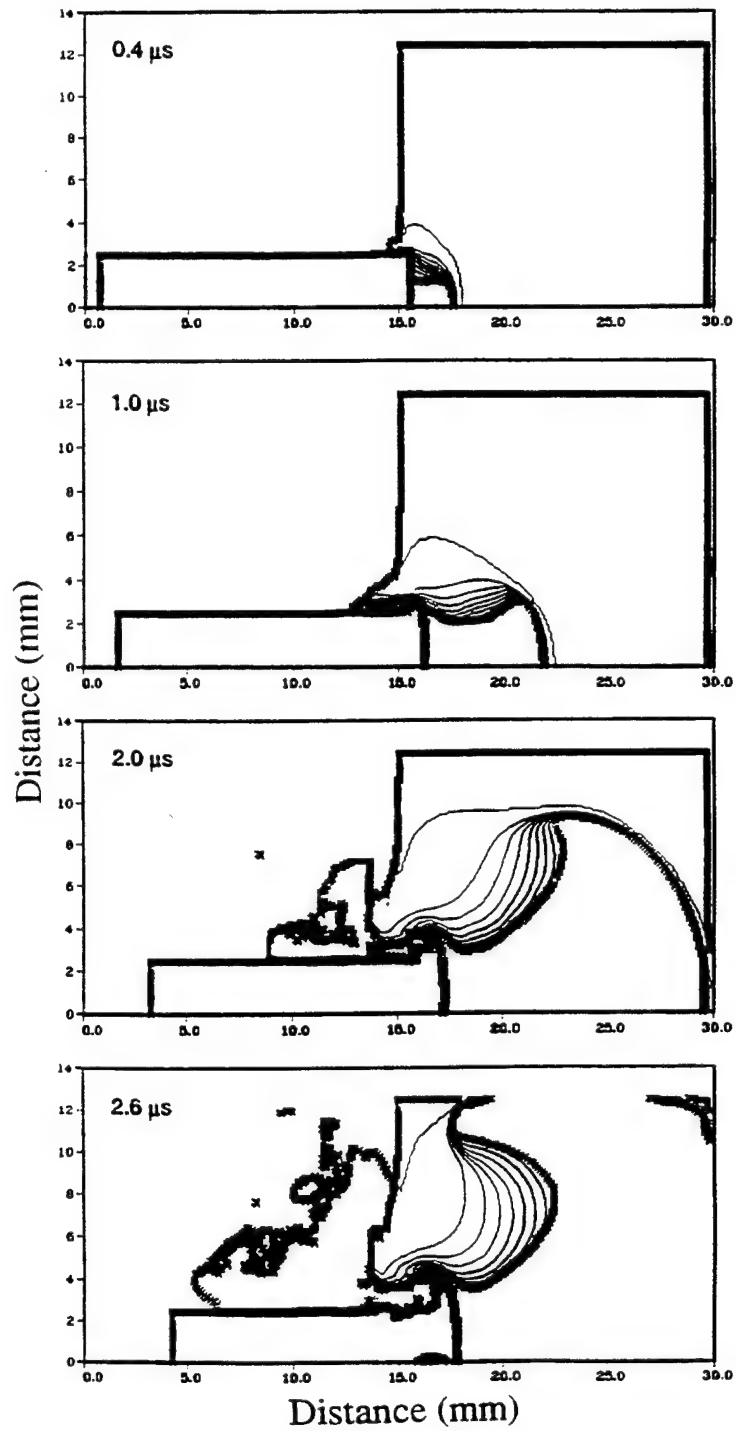
Figure 8. Mass fraction contour plots showing impact-mode initiation following the impact of 5.0-mm-diameter jet at 1.65 mm/µs.
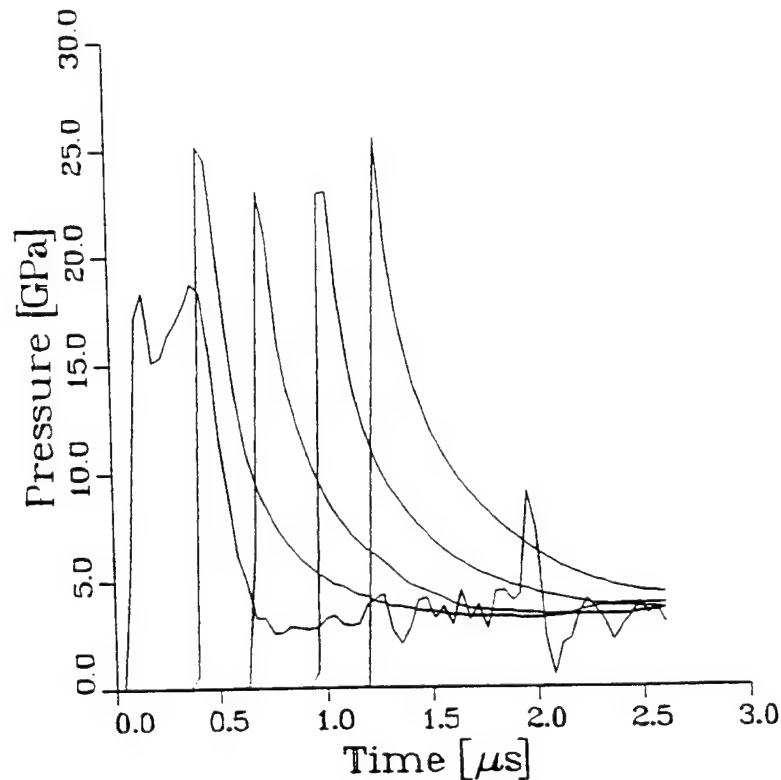
Figure 9. <u>Pressure history for impact-mode initiation with 5.0-mm-diameter jet at 1.65 mm/µs</u>.

projectile appears to have been carried to only 2.0 µs. This is considerably shorter than the times we needed to observe penetration-mode initiation. Thus, he may have identified a threshold between impact- and penetration-mode initiations.

5. CONCLUSIONS

We observed two modes of initiation associated with shaped-charge jet attack against bare Composition B. Prompt impact-mode initiation occurs for both subsonic and supersonic penetration. These results are consistent with Chick's [2] observations. Velocity thresholds for large subsonic jets agree with the Jacobs-Roslund fit. For jets with diameters smaller than the failure diameter of the explosive they attack, higher velocities than predicted by Jacobs-Roslund
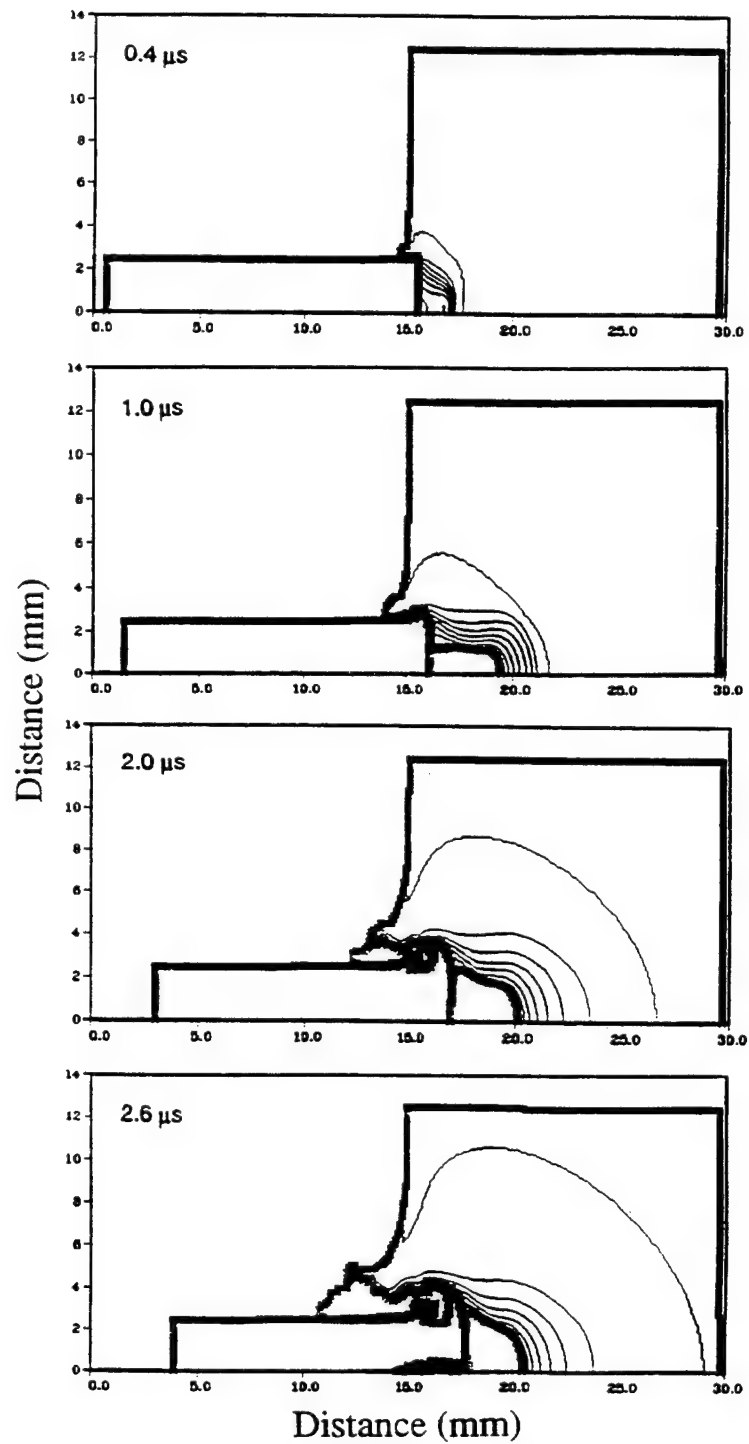
Figure 10. Mass fraction contour plots showing initiation failure following the impact of 5.0-mm-diameter jet at 1.5 mm/μs.

14

Table 1. Summary of Computational Results

Jet Diameter (mm)	Jet Velocity (km/s)	Penetration Velocity (km/s)	Initiation Mode
0.3	10.00		F
0.3	12.00		I
0.6	8.00	5.5–5.7	P
	10.00	6.8	I
1.0	7.50	5.1	P
	8.50	5.7	I
1.5	4.70		F
	5.00		P
	5.20		I
2.0	2.50	1.7	F
	3.10	2.1	I
5.0	1.50		F
	1.65		I
8.0	1.00		F
	1.15		P
12.0	0.90		P
	0.80		F

Note: Impact-mode initiation (I), initiation failure (F), penetration-mode initiation (P).

are required for initiation. A critical threshold between impact- and penetration-mode initiation was determined, but a similar threshold between penetration-mode initiation and initiation failure has not yet been determined due to limitations of the code. As assessment of the effects of stretching jets on penetration-mode initiation and initiation failure using the CTH code is planned.

Jet Velocity [mm/µs]

10^1

Sonic Penetration

10^0

× Initiation Failure
■ Impact-Mode Initiation
□ Penetration-Mode Initiation
+ Indeterminate Response
–·· Lundstrom [8]
— Jacobs-Roslund [$v^2 d = 10.6$ mm^3/µs^2]

$5*10^{-1}$

$5*10^{-2}$ 10^{-1} 10^0 10^1

d_j/d_f

Figure 11. Critical velocities as a function of the projectile diameter normalized with respect to the failure diameter.

16

6. REFERENCES

1. Roslund, L. A., J. W. Watt, and N. L. Coleburn. "Initiation of Warhead Explosives by the Impact of Controlled Fragments I: Normal Impact." NOLTR-73-124, Naval Ordnance Laboratory, White Oak, MD, August 1974.

2. Chick, M. C., I. B. Macintyre, and R. B. Frey. "The Jet Initiation of Solid Explosive." Proceedings of the Eighth Symposium (International) on Detonation, pp. 318–329, July 1985.

3. Frey, R. B., W. Lawrence, and M. C. Chick. "Shock Evolution After Shaped-Charge Jet Impact and Its Relevance to Explosive Initiation." International Journal of Impact Engineering, vol. 16, no. 4, pp. 563–570, 1995.

4. Kershner, J. D., and C. L. Mader. "2DE, A Two-Dimensional Continuous Eulerian Hydrodynamic Code for Computing Multicomponent Reactive Hydrodynamic Problems." LA-4846, Los Alamos Scientific Laboratory, Los Alamos, NM, 1972.

5. Mader, C. L. "An Empirical Model of Heterogeneous Shock Initiation of 9404." LA-4475, Los Alamos Scientific Laboratory, Los Alamos, NM, 1970.

6. Ramsey, J. B., and A. Popolato. "Analysis of Shock Wave and Initiation Data for Solid Explosives." Proceedings of the Fourth Symposium (International) on Detonation, pp. 233–238, 1965.

7. Starkenberg, J., Y. K. Huang, A. L. Arbuckle. "Numerical Modeling of Projectile Impact Initiation of Bare and Covered Composition B." BRL-TR-02576, U.S. Army Ballistic Research Laboratory, Aberdeen Proving Ground, MD, 1984.

8. Lundstrom, E. A. "Evaluation of Forest Fire Burn Model of Reaction Kinetics of Heterogeneous Explosives." Technical Publication 6898, Naval Weapons Center, White Oak, MD, 1988.

INTENTIONALLY LEFT BLANK.

APPENDIX:

MASS FRACTION CONTOUR PLOTS

INTENTIONALLY LEFT BLANK.

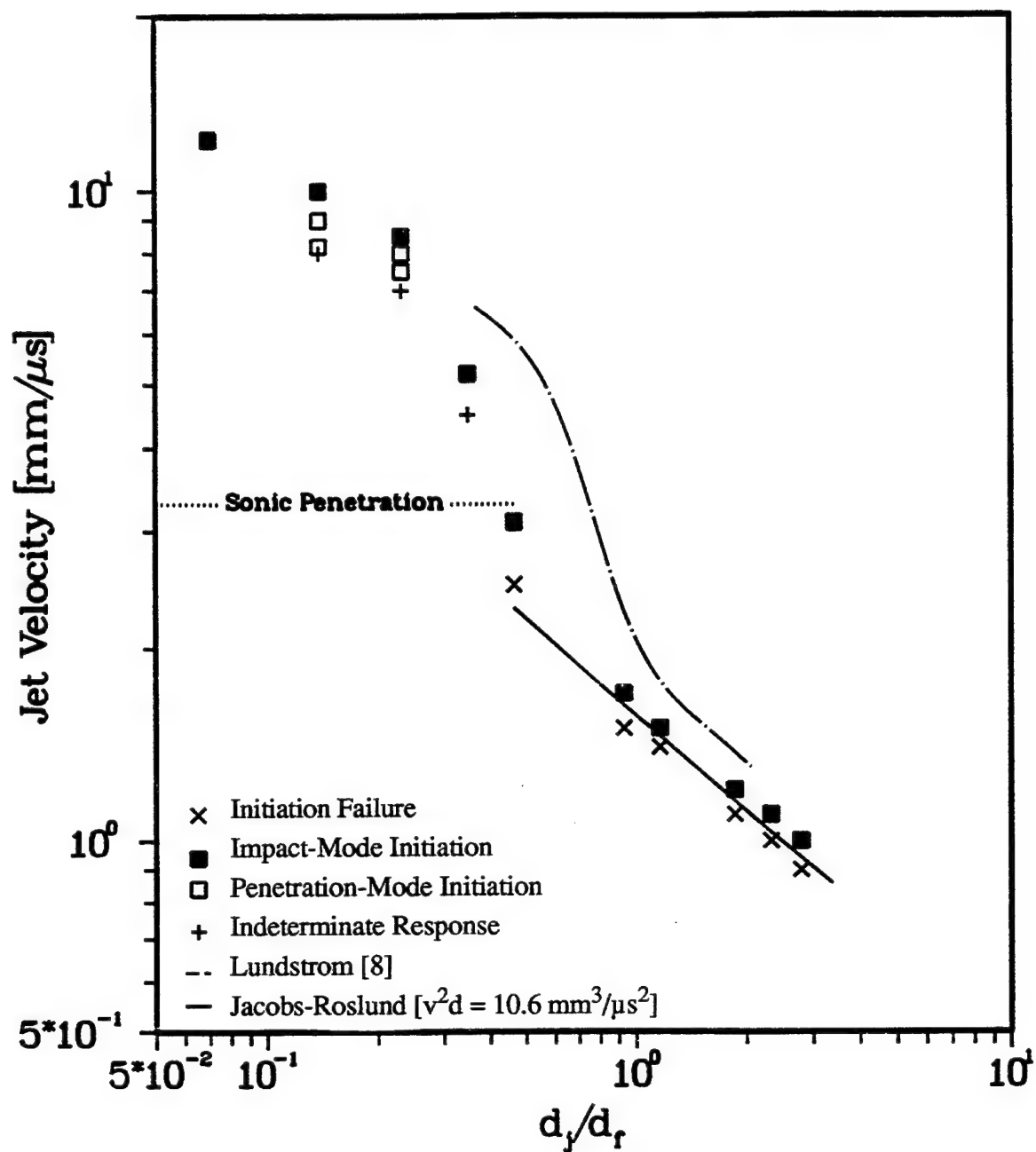$d_j = 0.6$ mm (below failure) $v_j = 10.0$ mm/μs (supersonic penetration)

Figure A-1. Mass fraction contour plots showing impact-mode initiation following the impact of 0.6-mm-diameter jet at 10.0 mm/μs.

21

$d_j = 0.6$ mm (below failure) $v_j = 8.2$ mm/μs (supersonic penetration)
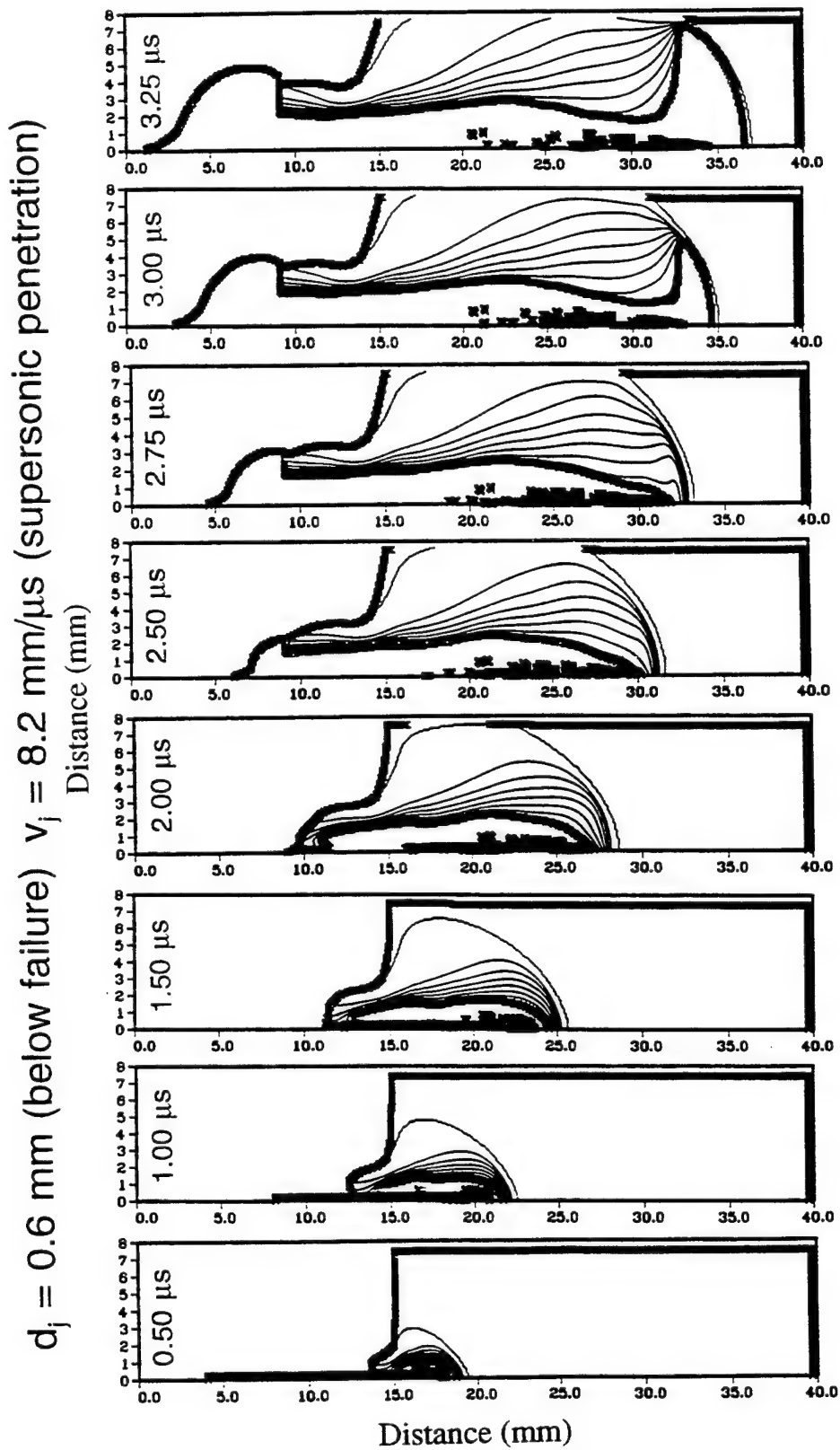
Figure A-2. Mass fraction contour plots showing penetration-mode initiation following the impact of 0.6-mm-diameter jet at 8.2 mm/μs.

22

$d_j = 0.6$ mm (below failure) $v_j = 8.0$ mm/µs (supersonic penetration)
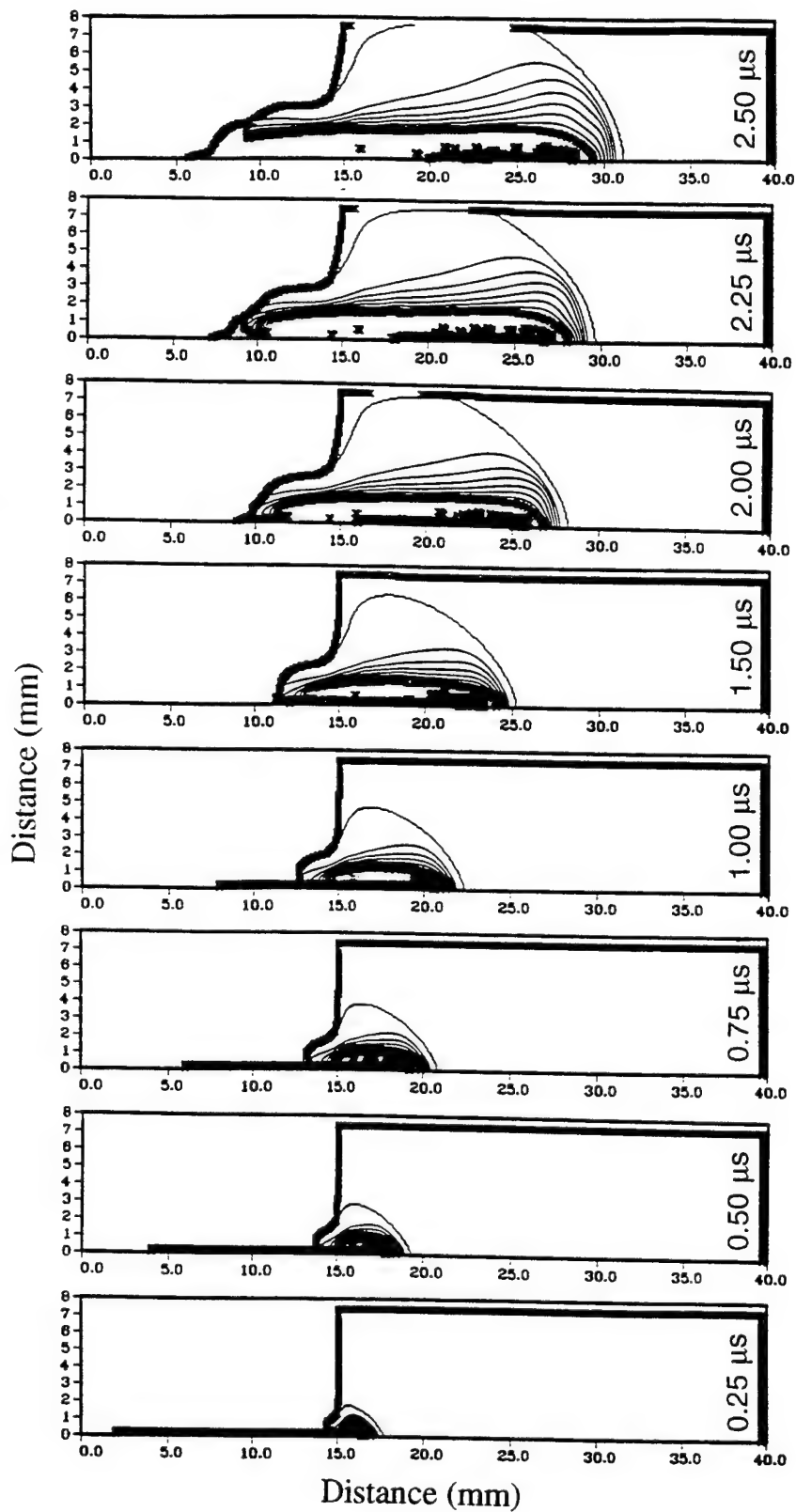
Figure A-3.   Mass fraction contour plots showing the indeterminate response following the impact of 0.6-mm-diameter jet at 8.0 mm/µs.

23

$d_j = 4.0$ mm (near failure) $v_j = 1.7$ mm/µs (subsonic penetration)

Distance (mm)

Distance (mm)

Figure A-4. Mass fraction contour plots showing impact-mode initiation following the impact of 4.0-mm-diameter jet at 1.7 mm/µs.

24

$d_j = 4.0$ mm (near failure) $v_j = 1.5$ mm/µs (subsonic penetration)
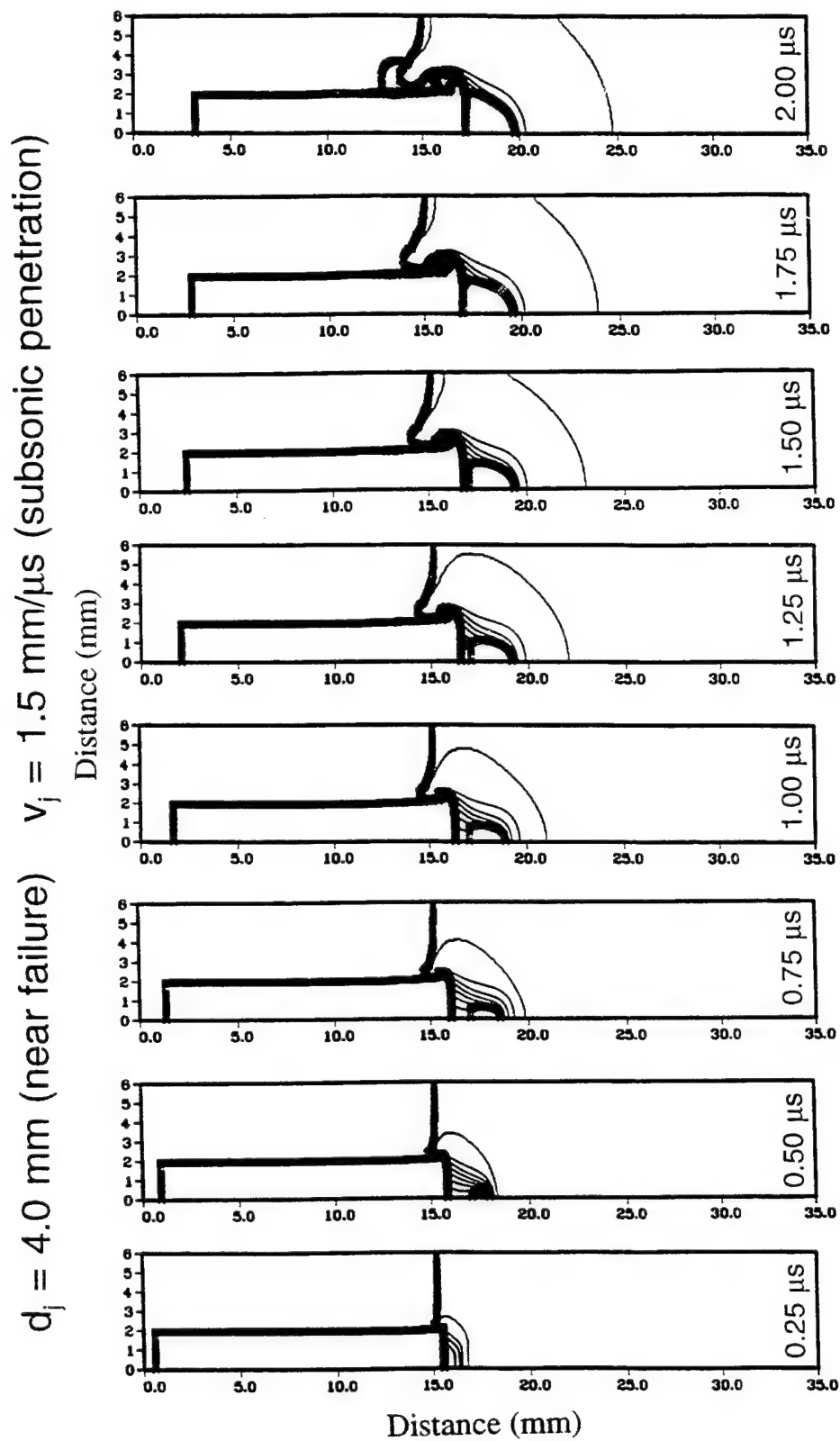
Figure A-5.   Mass fraction contour plots showing initiation failure following the impact of 4.0-mm-diameter jet at 1.5 mm/µs.
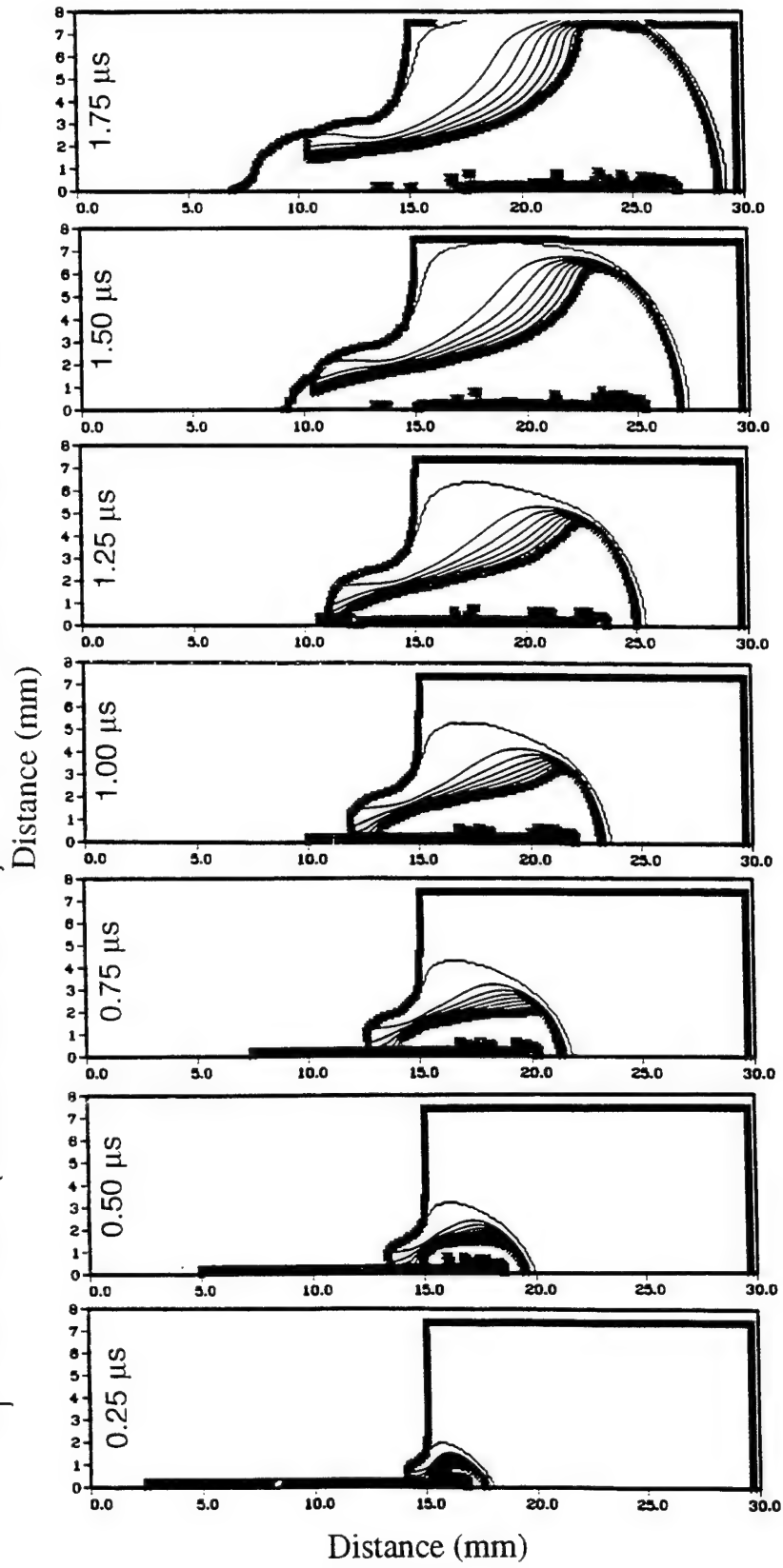
25
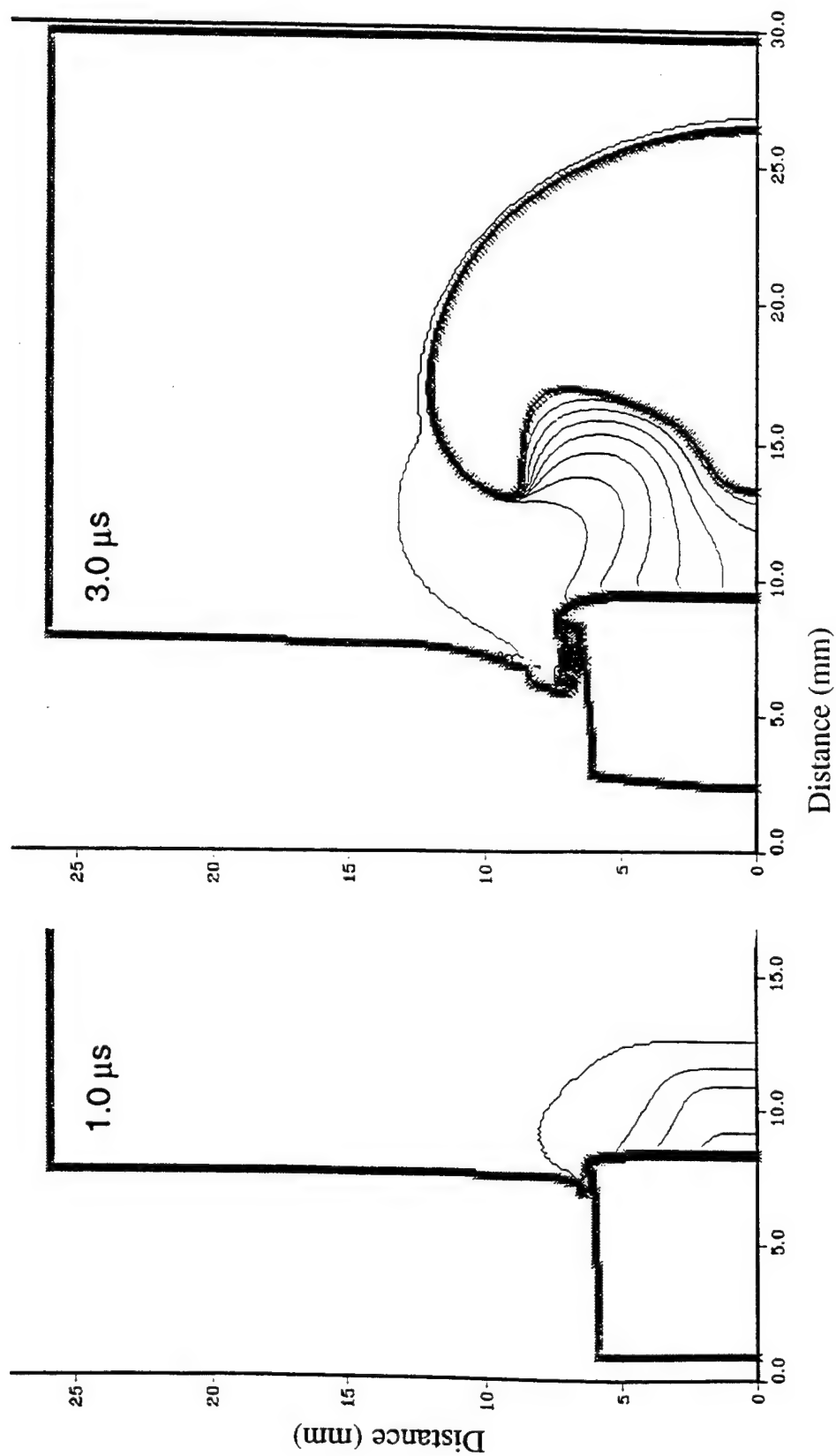
Figure A-6. Mass fraction contour plots showing impact-mode initiation following the impact of 12.0-mm-diameter jet at 0.9 mm/μs.

26
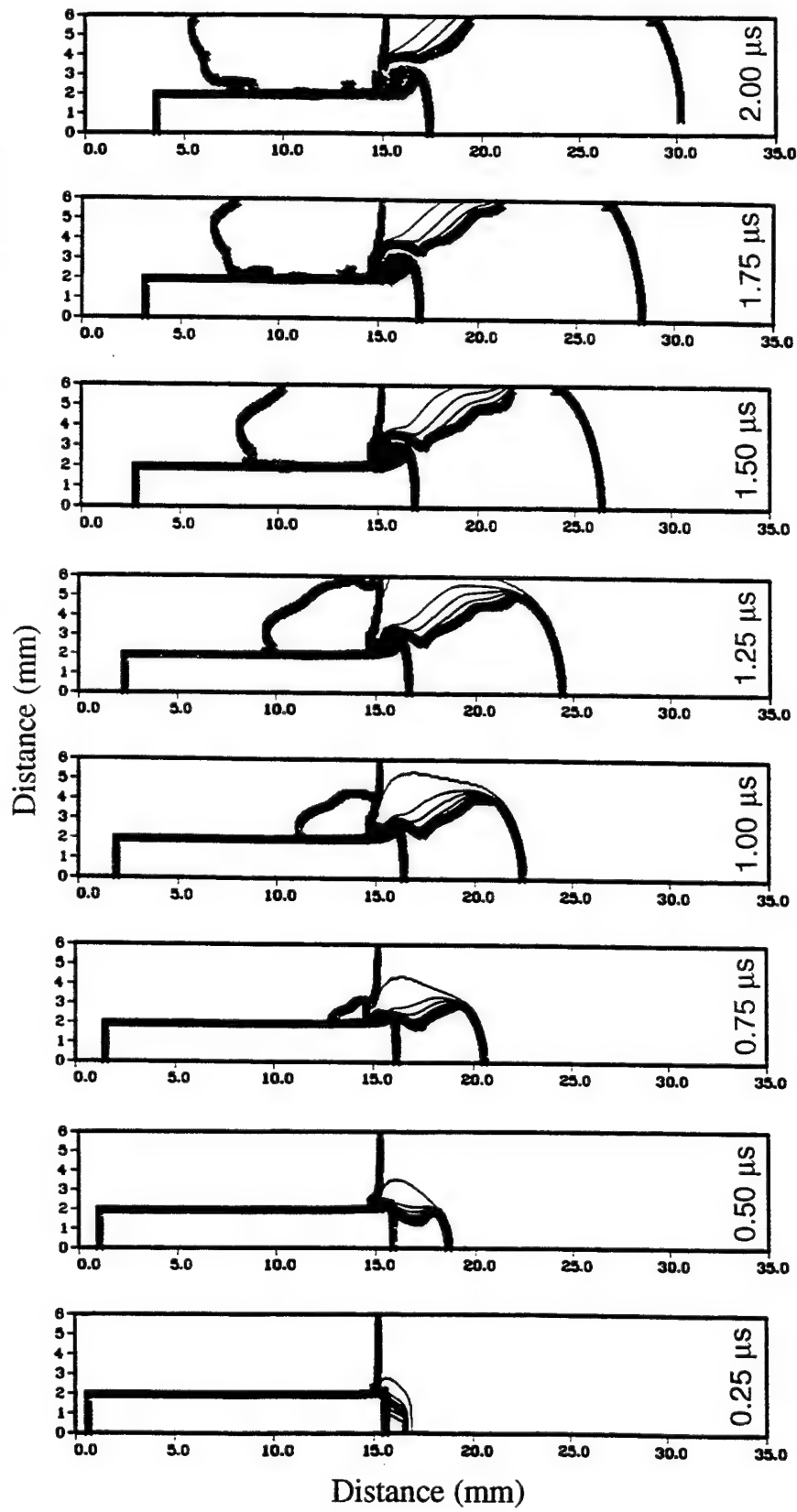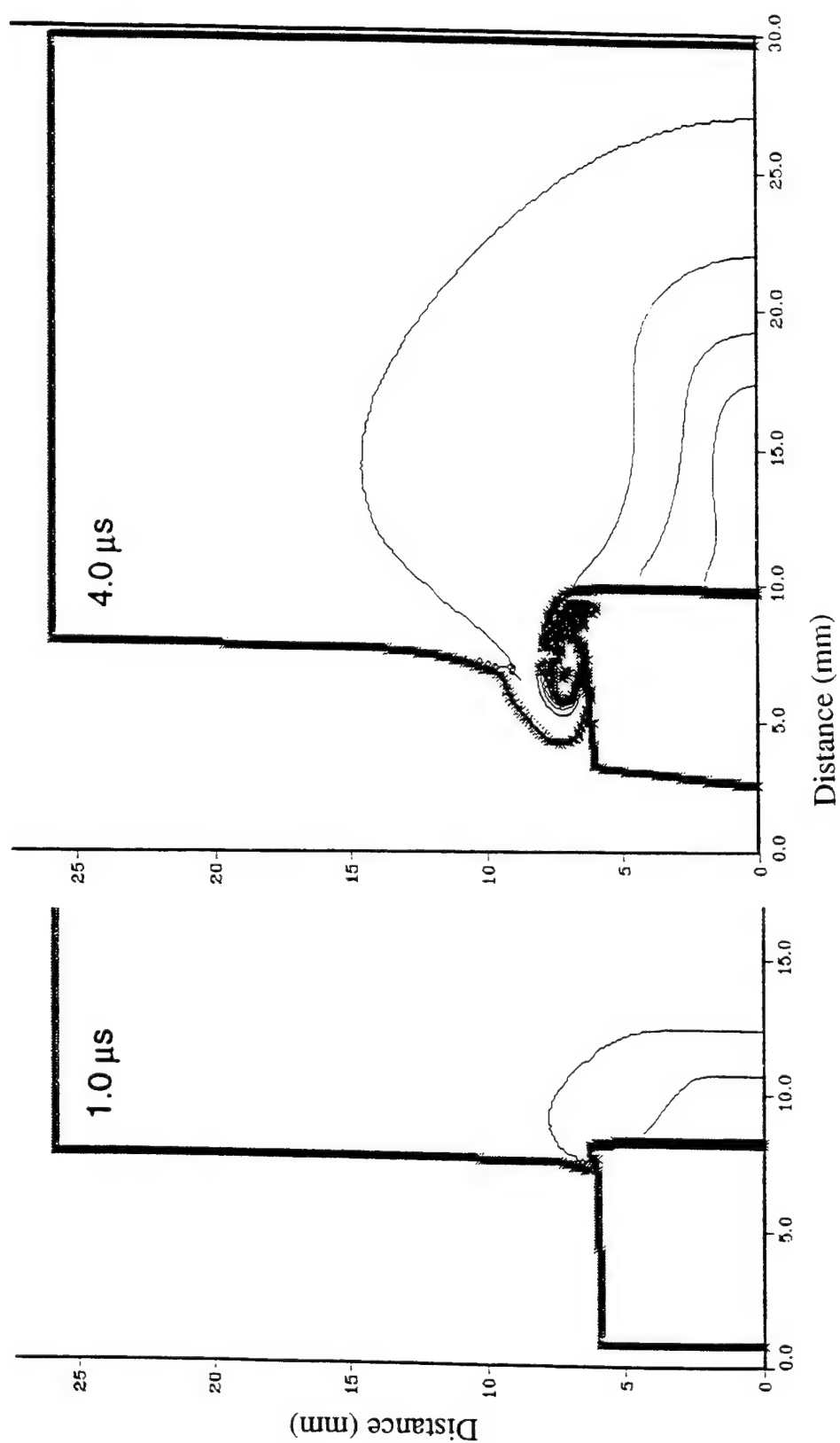
Figure A-7. Mass fraction contour plots showing initiation failure following the impact of 12.0-mm-diameter jet at 0.8 mm/µs.

27

INTENTIONALLY LEFT BLANK.

NO. OF
COPIES   ORGANIZATION

2   DEFENSE TECHNICAL INFO CTR
     ATTN DTIC DDA
     8725 JOHN J KINGMAN RD
     STE 0944
     FT BELVOIR VA 22060-6218

1   HQDA
     DAMO FDQ
     ATTN DENNIS SCHMIDT
     400 ARMY PENTAGON
     WASHINGTON DC 20310-0460

1   US MILITARY ACADEMY
     MATH SCI CTR OF EXCELLENCE
     DEPT OF MATHEMATICAL SCI
     ATTN MDN A MAJ DON ENGEN
     THAYER HALL
     WEST POINT NY 10996-1786

1   DIRECTOR
     US ARMY RESEARCH LAB
     ATTN AMSRL CS AL TP
     2800 POWDER MILL RD
     ADELPHI MD 20783-1145

1   DIRECTOR
     US ARMY RESEARCH LAB
     ATTN AMSRL CS AL TA
     2800 POWDER MILL RD
     ADELPHI MD 20783-1145

3   DIRECTOR
     US ARMY RESEARCH LAB
     ATTN AMSRL CI LL
     2800 POWDER MILL RD
     ADELPHI MD 20783-1145

     ABERDEEN PROVING GROUND

2   DIR USARL
     ATTN AMSRL CI LP (305)

29

NO. OF
COPIES   ORGANIZATION

ABERDEEN PROVING GROUND

20   DIR, USARL
        ATTN: AMSRL-WM-T, W. MORRISON
                AMSRL-WM-TA,
                    W. BRUCHEY
                    J. DEHN
                    W. GILLICH
                    T. HAVEL
                    J. RUNYEON
                    M. ZOLTOSKI
                AMSRL-WM-TB,
                    K. BENJAMIN
                    V. BOYLE
                    P. BAKER
                    T. DORSEY
                    R. FREY
                    W. HILLSTROM
                    W. LAWRENCE
                    J. STARKENBERG
                    J. WATSON
                AMSRL-WM-TC, W. DE ROSSET
                AMSRL-WM-TD,
                    A. DIETRICH, JR.
                    A. GUPTA
                    D. PRITCHARD

REPORT DOCUMENTATION PAGE

Public reporting burden for this collection of information is estimated to average 1 hour per response, including the time for reviewing instructions, searching existing data sources, gathering and maintaining the data needed, and completing and reviewing the collection of information. Send comments regarding this burden estimate or any other aspect of this collection of information, including suggestions for reducing this burden, to Washington Headquarters Services, Directorate for Information Operations and Reports, 1215 Jefferson Davis Highway, Suite 1204, Arlington, VA 22202-4302, and to the Office of Management and Budget, Paperwork Reduction Project(0704-0188), Washington, DC 20503.

1. AGENCY USE ONLY *(Leave blank)*	2. REPORT DATE April 1997	3. REPORT TYPE AND DATES COVERED Final, Jul 92 - Dec 95

4. TITLE AND SUBTITLE	5. FUNDING NUMBERS
The Effects of the Failure Diameter of an Explosive on Its Response to Shaped-Charge Jet Attack	78T8FC

6. AUTHOR(S)

William Lawrence and John Starkenberg

7. PERFORMING ORGANIZATION NAME(S) AND ADDRESS(ES)	8. PERFORMING ORGANIZATION REPORT NUMBER
U.S. Army Research Laboratory ATTN: AMSRL-WM-TB Aberdeen Proving Ground, MD 21005-5066	ARL-TR-1350

9. SPONSORING/MONITORING AGENCY NAMES(S) AND ADDRESS(ES)	10.SPONSORING/MONITORING AGENCY REPORT NUMBER

11. SUPPLEMENTARY NOTES

12a. DISTRIBUTION/AVAILABILITY STATEMENT	12b. DISTRIBUTION CODE
Approved for public release; distribution is unlimited.	

13. ABSTRACT *(Maximum 200 words)*

In order to shed some light on the response of explosives to the attack of small-diameter projectiles such as shaped-charge jets, a computational study using the 2DE code and the Forest Fire explosive initiation model for Composition B was conducted. In our computations we modeled the jet as a cylindrical projectile with a flat end that moves without stretching. Jet attack simulations were run in order to determine modes of initiation and critical velocity for initiation as a function of jet diameter. The diameter of the jet was varied between 0.3 and 12.0 mm. The velocity of the jet was varied between 0.8 and 15.0 km/s. The target diameter was at least three times the jet diameter, and the target was between 4 and 60 jet diameters deep. Two modes of initiation associated with shaped-charge jet attack were observed. Prompt impact-mode initiation occurred for both subsonic and supersonic penetration. Delayed penetration-mode initiation occurred only for supersonic penetration. The velocity threshold for large subsonic jets agreed with the Jacobs-Roslund fit. For jets with diameters smaller than the failure diameter of the explosive they attack, higher velocities than predicted by Jacobs-Roslund were required for initiation. A critical boundary between impact- and penetration-mode initiation was determined over the entire supersonic range. A similar boundary between penetration-mode initiation and initiation failure for 0.3-mm and 1.5-mm-diameter jets was found, but the initiation failure threshold for other jet diameters has not yet been determined.

14. SUBJECT TERMS				15. NUMBER OF PAGES
projectile, shaped-charge jets, impact initiation of explosive, modes of initiation, 2DE code, forest fire model				33
				16. PRICE CODE

17. SECURITY CLASSIFICATION OF REPORT	18. SECURITY CLASSIFICATION OF THIS PAGE	19. SECURITY CLASSIFICATION OF ABSTRACT	20. LIMITATION OF ABSTRACT
UNCLASSIFIED	UNCLASSIFIED	UNCLASSIFIED	UL

NSN 7540-01-280-5500

Standard Form 298 (Rev. 2-89)
Prescribed by ANSI Std. 239-18   298-102

INTENTIONALLY LEFT BLANK.

USER EVALUATION SHEET/CHANGE OF ADDRESS

This Laboratory undertakes a continuing effort to improve the quality of the reports it publishes. Your comments/answers to the items/questions below will aid us in our efforts.

1. ARL Report Number/Author ___ARL-TR-1350 (Lawrence)___ Date of Report ___April 1997___

2. Date Report Received _____

3. Does this report satisfy a need? (Comment on purpose, related project, or other area of interest for which the report will be used.) _____

_____

_____

4. Specifically, how is the report being used? (Information source, design data, procedure, source of ideas, etc.) _____

_____

_____

5. Has the information in this report led to any quantitative savings as far as man-hours or dollars saved, operating costs avoided, or efficiencies achieved, etc? If so, please elaborate. _____

_____

_____

6. General Comments. What do you think should be changed to improve future reports? (Indicate changes to organization, technical content, format, etc.) _____

_____

_____

_____

CURRENT
ADDRESS

Organization _____

Name _____ E-mail Name _____

Street or P.O. Box No. _____

City, State, Zip Code _____

7. If indicating a Change of Address or Address Correction, please provide the Current or Correct address above and the Old or Incorrect address below.

OLD
ADDRESS

Organization _____

Name _____

Street or P.O. Box No. _____

City, State, Zip Code _____

(Remove this sheet, fold as indicated, tape closed, and mail.)
(DO NOT STAPLE)

DEPARTMENT OF THE ARMY

OFFICIAL BUSINESS

BUSINESS REPLY MAIL
FIRST CLASS PERMIT NO 0001,APG,MD

POSTAGE WILL BE PAID BY ADDRESSEE

DIRECTOR
US ARMY RESEARCH LABORATORY
ATTN AMSRL WM TB
ABERDEEN PROVING GROUND MD 21005-5066

NO POSTAGE
NECESSARY
IF MAILED
IN THE
UNITED STATES